

## An automated dye-dilution based seepage meter for the time-series measurement of submarine groundwater discharge

Edward Sholkovitz, Craig Herbold, and Matthew Charette<sup>1</sup>

Department of Marine Chemistry and Geochemistry, Woods Hole Oceanographic Institution, Woods Hole, Massachusetts 02543

### Abstract

We designed an automated seepage meter that can detect and quantify both groundwater outflow and seawater infiltration. Based on a dye-dilution technique, this instrument provides high-resolution time-series data for submarine groundwater discharge to the coastal zone. The dye-dilution method involves two repeatable steps: (1) the timed injection of a water-soluble dye into a “dye-mixing chamber” mounted in series with a seepage chamber and (2) the subsequent timed measurements of the absorbance of the dyed solution. The rate at which the dyed solution is diluted by the inflow or outflow of water is directly proportional to the flow rate moving through the surface area of the seepage housing. In addition to describing the instrument’s components and the operating principle, we provide examples of laboratory flow calibrations and field deployments. As indicated by two sets of time-series studies, this instrument has performed reliably in field tests at Waquoit Bay (Cape Cod, Massachusetts) and Shelter Island (Long Island, New York). The instrument has yielded hydrologically consistent flow rates and has revealed major and subtle connections between tidal stage and the rate and direction of submarine groundwater discharge.

Submarine groundwater discharge (SGD) has received increased attention as a potential source for the oceanic budgets of certain chemical species (Moore 1996, 1999; Moore and Shaw 1998; Shaw et al. 1998; Basu et al. 2001). Though the uncertainties of global SGD at present are too large to make definitive statements with respect to ocean budgets (Burnett et al. 2001, 2002), local inputs of nutrient-rich groundwater are common throughout the world and can represent a significant fraction of the freshwater supply of nutrients to salt marshes, coastal waters, bays, and coral reefs (Johannes 1980; Johannes and Hearn 1985; Zimmerman et al. 1985; Lewis 1987; Reay et

al. 1992; Simmons 1992; Millham and Howes 1994; Li et al. 1999; Rutkowski et al. 1999; Krest et al. 2000; Montlucon and Sanudo-Wilhelmy 2001; Tobias et al. 2001). SGD-derived nutrient inputs to coastal waters can lead to environmental problems, in particular eutrophication and the deterioration of the natural ecology (Valiela et al. 1990, 1992). Hence, the physics and biogeochemistry of SGD represent important areas of research within coastal oceanography (Moore 1996, 1999; Bokuniewicz 2001; Burnett et al. 2001, 2002).

The term “submarine groundwater discharge” has been used in the literature to describe the upward flow of water into the ocean from the sediments (Moore 1996, 1999). Depending on the geology and hydrology of the study site, SGD can be totally fresh (groundwater), brackish, or fully saline (recirculated seawater). Brackish SGD indicates entrainment of seawater into the upward flowing freshwater. In addition to the flow from coastal sediments, the change in sea level (due to tides) relative to the water table elevation can lead to a reversal of the flow direction whereby seawater flows into the sediments from the overlying water (Paulsen et al. 2001). In this article, we use the term “outflow” to refer to the seepage of water from the sediment to the overlying water column. “Inflow” will refer to the flow from the water column into the sediment; the term “reverse flow” has also been applied to this direction of flow (Paulsen et al. 2001).

Though the overall importance of SGD in the coastal ocean is well known, there exists less information on the mechanism

<sup>1</sup>Corresponding author (mcharette@whoi.edu)

### Acknowledgments

We thank William Burnett and Henry Bokuniewicz for inviting us to participate in the Shelter Island intercomparison experiment sponsored by Working Group 112 (*Magnitude of Submarine Groundwater Discharge and Its Influence on Coastal Oceanographic Processes*) of the Scientific Committee on Oceanic Research (SCOR). We extend our continued appreciation to the director and staff of the Waquoit Bay National Estuarine Research Reserve for allowing and encouraging us to use Waquoit Bay as our study site. Kevin Kroeger and Peter Statham provided valuable comments on a draft version. Three journal reviewers provided rapid and valuable comments. Matt Allen assisted in the field, and Mike Purcell and Mark St. Pierre provided engineering expertise. Development of the seepage meter was supported with funding from the NOAA Cooperative Institute for Coastal and Estuarine Environmental Technology at the University of New Hampshire, grants NA07OR0351-01-469 and NA17OZ2507-03-723. This article is WHOI contribution #10891.

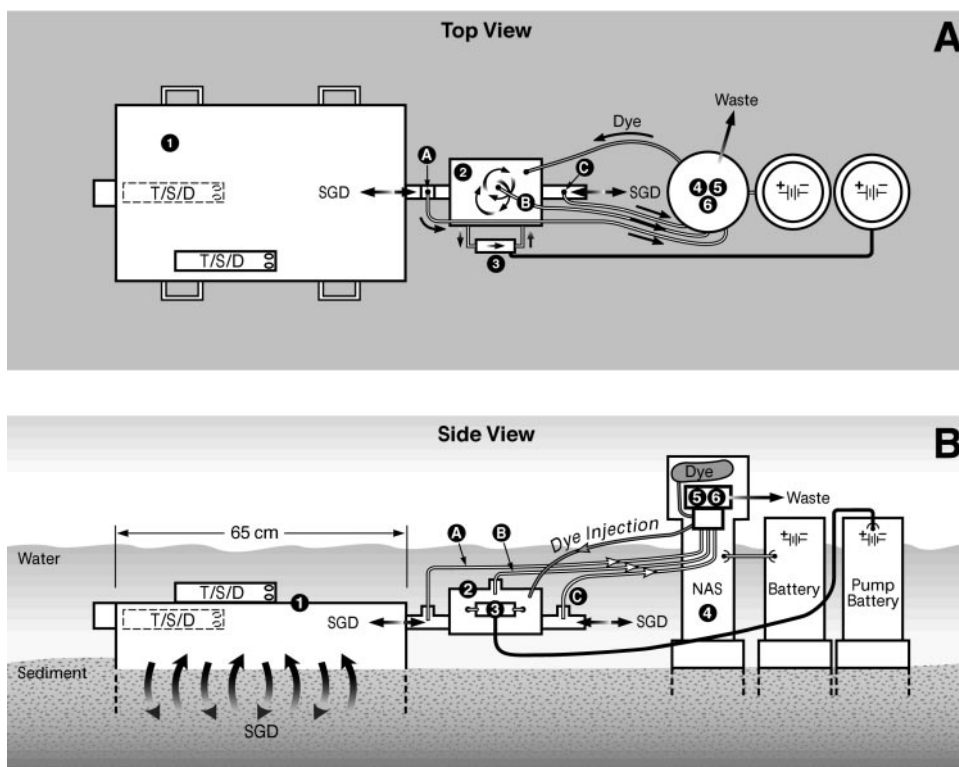


**Fig. 1.** A schematic diagram of the automated seepage meter in A) top view and B) side view. The four main components of the instrument are a seepage housing (1), a dye-mixing chamber (2), a battery-operated submersible pump (3), and a battery-operated WS EnviroTech Ltd. model NAS-2E in situ nutrient analyzer (4), which has been used to inject the dye and make absorbance measurements. Label 5 is an eight-way injection port and syringe, and label 6 is a spectrophotometer. Two in situ probes to record internal and external temperature (T), salinity (S), and depth (D) are shown inside and outside of the seepage housing. Labels A, B, and C are the sampling ports at which the solution absorbances are measured by the spectrophotometer.

of SGD and how it relates to external forcing functions, such as changes in sea level, tides, aquifer recharge, and sediment permeability (Robinson et al. 1998; Uchiyama et al. 2000; Taniguchi and Iwakawa 2001; Taniguchi 2002). To this end, we designed, built, and tested an automated seepage meter that can measure the rate of water flow across the sediment-water interface in either direction. Based on a dye-dilution technique, this instrument can provide high-resolution time-series data for submarine groundwater discharge to the coastal zone. This instrument has performed reliably in field tests at Waquoit Bay (Cape Cod, Massachusetts) and Shelter Island (Long Island, New York).

Acoustic and heat-pulse seepage meters provide the same type of measurements (Taniguchi and Fukuo 1993; Krupa et al. 1998; Paulsen et al. 2001; Taniguchi and Iwakawa 2001). Our instrument offers the community an alternative technology with certain advantages. With respect to the dye-dilution method, the underlying principles and electronics of the heat-pulse and the acoustic methods are much more complex. Hence, expertise in fairly complex physics and electronics are needed to maintain these instruments. Unlike the other two instruments, the dye-dilution method can be operated in both an autonomous and a manual mode. Whereas this article

focuses on the fully autonomous mode of operation, we also describe the manual option, which requires the injection of dye and the measurement of absorbance from hand-drawn samples. Additionally, salinity probes in our seepage meter allow one to estimate the relative amounts of freshwater and saltwater associated with SGD. While the instrument application in this article will center on SGD to the coastal ocean, our seepage meter can be employed in other aquatic systems such as lakes.

### Materials and procedures

Our instrument is shown in schematic form in Fig. 1. Photographs of the instruments are presented in Figs. 2 and 3. We use a dye-dilution technique to measure the rates of inflow and outflow. The dye-dilution method involves two repeatable steps: 1) the timed injection of a water-soluble dye into a “dye-mixing chamber” mounted in stream with a seepage housing and 2) the subsequent timed measurements of the absorbance of the dyed solution. The rate at which the dyed solution is diluted by the inflow or outflow of water is directly proportional to the flow rate through the surface area of the sediment under the seepage housing.

*Materials*—There are four major components to our instrument (Fig. 1–3). The first component is a seepage housing that



**Fig. 2.** The automated seepage meter showing all major components of the system except for the seepage housing.

is pushed into the sediment. This housing is modeled after the one used by Paulsen et al. (2001) and funnels water moving vertically through  $0.286 \text{ m}^2$  of sediment into the dye-mixing chamber. This design was chosen over the traditional Lee-type 55-gallon drum housing (Lee 1977) for its low profile that allows for deployment in shallow waters (e.g., during low tide along the seepage face). The bottom of the housing is  $65 \text{ cm} \times 44 \text{ cm}$  and the four sides of the housing are 15 cm high. The roof of the housing tapers slightly and reaches a peak at 17 cm above the bottom of the housing. The depth to which the housing is pushed into the sediment will determine the head-space volume of the overlying water; this volume ranges from 15 to 30 L.

The second component, connected onto the seepage housing on the seaward side, is referred to as the “dye-mixing chamber.” The dilution of a dyed solution by the outflow or inflow of water takes place in this chamber. We have employed both a small (internal volume = 544 mL) and a large (2370 mL) dye-mixing chamber, depending on the rate of dilution (i.e., seepage rate) at a specific site. The small mixing chamber was machined from a polypropylene block with approximate outside (inside) dimensions of 25 (22) cm long, 8 (5.5) cm wide, and 5 (3.5) cm high. The top consists of a clear plastic plate with an o-ring seal. Pipe fittings (1/4 in) were threaded into the walls of the chamber and are used for the inlets and outlets to carry the recirculating water, dyed solutions and SGD (Fig. 1). The larger mixing chamber was modified from a Rose enclosure box with a watertight seal. The outside (inside) dimensions are approxi-

mately 26 (23) cm long, 16 (13) cm wide, and 9 (7) cm high. The same pipe fittings were employed on the large chamber.

The third component is a battery-driven submersible pump (Sea Bird Model SBE 5M) that serves to recirculate water within the dye-mixing chamber. The dye-dilution method requires that there be rapid mixing of the dyed solution with water that is flowing in or out during the deployment period. The SBE 5M submersible pump does this job quickly (<15 s) and reliably. Our laboratory experiments have shown that operating the pump does not alter the flow rate of water into and out of the dye-mixing chamber.

The fourth component is a battery-operated, in situ nutrient analyzer (WS EnviroTech Ltd. model NAS-2E), which we have modified to inject the dye and make absorbance measurements. The NAS-2E analyzer was designed by the manufacturer to measure nitrate in seawater for periods of days to weeks. The NAS nitrate analyzer contains a spectrophotometer optimized to measure the absorbance of a solution at 560 nm in a 1- or 2-cm flow-through cell. The NAS analyzer also contains an eight-port manifold that is connected to a mechanically operated syringe. In the nitrate-analyzing mode, these ports are used to mix color-forming reagents with a seawater sample in the syringe, followed by an absorbance measurement in the spectrophotometer cell. As shown in Fig. 1, we have used the port/syringe system (label 5) and the spectrophotometer (label 6) of the NAS-2E to inject dye into the dye-mixing chamber and measure the absorbance of the water in three locations: (1) the dye-mixing chamber (B in Fig. 1), (2) the mixing chamber inlet (A in Fig. 1), and (3) the mixing chamber outlet (C in Fig. 1).

By measuring the absorbance at these three locations, our instrument is capable of quantifying flow in two directions. While the dye-dilution measurements are recorded at location B, measurements made at locations A and C provide the background absorbance of the inflow and outflow of water relative

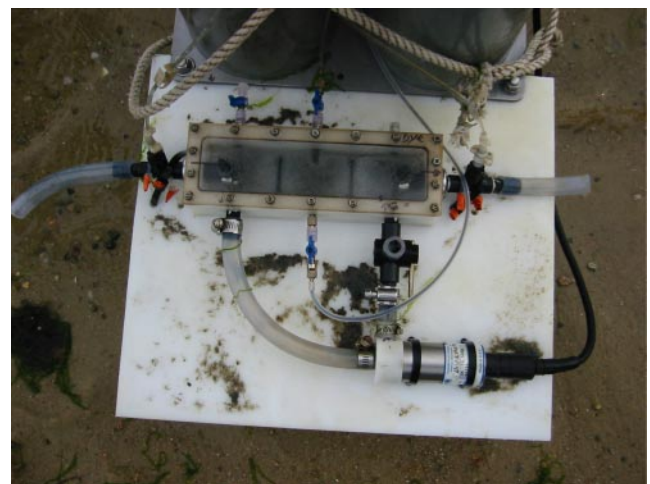


**Fig. 3.** Close-up of the dye-mixing chamber and the battery-operated submersible pump.

to the dye-mixing chamber. Obtaining background absorbance data is a critical part of the dye-dilution method as this information indicates the direction of flow. For example, under conditions of outflow, water in the seepage housing will move in the direction of A to C. In this scenario, absorbance values at location A are relatively low, and therefore provide the background absorbance data for the absorbance measurements made at location B; absorbance values at location C would be relatively high and track the absorbance values from location B, indicating seepage outflow. The rate of outflow can be calculated by measuring the change in the absorbance of water inside the dye-mixing chamber as function of time, corrected for the background absorbance of seepage water flowing out.

Under conditions of inflow, seawater will move into the dye-mixing chamber, forcing the dyed water into the seepage housing and sediment. Sampling location C will provide the background absorbance of the inflowing seawater. Absorbance data at location A will show if and when the dyed water is moving into the seepage housing. The rate of inflow can be calculated by measuring the change in absorbance in the dye-mixing chamber as a function of time, corrected for the background absorbance of inflowing seawater. As discussed later, problems in interpreting the absorbance data can arise when dyed water in the seepage housing (from a period of inflow) flows back toward the mixing chamber and water column.

We use a bluish violet dye (External D&C Violet No. 2), produced by Warner Jenkinson of St. Louis. This anthraquinone-based dye goes by the common name Alizuro Purple SS. With its maximum absorption at 588 nm, the spectral properties of this dye closely match the optimal performance of the nitrate NAS-2E spectrophotometer at 560 nm. A measurement at 560 nm falls on a relatively flat part of the dye's adsorption curve. The dye is water-soluble and does not adhere to the sides of the dye-mixing chamber. Our laboratory studies show that the dye is stable in freshwater, brackish water, and seawater; the absorbances of these solutions remain constant for a least 36 hr. No flocculation of the dye has been observed. As explained later, long term (more than a few hours) stability of the dye is not a necessary condition for the dye-based method.

The operator needs to adjust the concentration of the dye solution according to the volume of the dye-mixing chamber. The objective is to have a strong initial absorbance signal for the dyed solution without exceeding the linear response (Beer's Law) range of the spectrophotometer. Absorbance values below 0.7, relative to distilled water, are in the linear range. In the case of our 544-mL dye-mixing chamber, we injected 3 mL of dye solution with a concentration of 0.6 g of powdered dye in 100 mL of deionized water.

*Flow calculation*—There are three ways to use the absorbance data to calculate the flow rates for the dye dilution method. The first method, which we used to process our long time-series data, employs a curve-fitting routine to determine flow rates from the absorbance measurements. In this approach, the exponential decay equation substitutes as an exponential dilution equation:

$$A_t = A_0 e^{-kt} \quad (1)$$

$A_t$ , the absorbance of dye in the mixing chamber at time  $t$ , is as a function of initial absorbance ( $A_0$ ) and a dilution rate constant ( $-k$ ) multiplied by time since dye injection ( $t$ ). The dilution rate constant ( $k$ ) is equal to the flow rate ( $r$ ) divided by the internal volume ( $V$ ) of the mixing chamber ( $k = r/V$ ). The dilution rate constant represents the throughput of water relative to the total mixing chamber volume at any given time. Thus, the solution for flow rate ( $r$ , mL min<sup>-1</sup>) using this method is the inverse slope of  $\ln(A)$  versus time multiplied by the mixing chamber volume ( $V$ ). Error on the flow value can be obtained by calculating multiple slopes from the same time period. The multiple slopes are treated as replicate measurements where the average value is used in calculating flow and the standard deviation represents error.

The dye-dilution method only relies on measuring the relative change in absorbance (Eq. 1). We typically inject dye once an hour and measure the change of absorbance over a period of 15 to 30 min. Hence, each individual flow measurement is short and independent of each other because the dye-dilution method is reset on an hourly basis. As long as the dyed-solution behaves conservatively over a period of an hour, the initial absorbance after each injection can vary. As explained later, the frequency of injection can be varied by the user. Problems in interpreting the absorbance data can arise when dyed water moves from the mixing chamber into the seepage housing, and then back into the mixing chamber and out to sea. This reversal of flow direction occurs at sites such as Waquoit Bay where the interplay between tidal height and water table elevation lead to a cycle of inflow and outflow. Depending on the relative flow rates and on the injection frequency of dye, there can be a buildup of dye in the headspace water within the seepage housing. However, these effects are minimized due to the dilution of dye in the relatively large volume of water in the headspace (15–30 L). At sites with a tidal reversal of SGD direction, it is important to measure the background absorbance values at the outlet and inlet ports prior to and during the injection and analysis cycle. If dye builds up to unacceptably high concentrations in the seepage housing, then it may not be possible to correct the absorbances recorded in the dye-mixing chamber. Because the headspace water is not stirred, there is no way to predict the absorbance of the dye-affected water exiting the housing to the mixing chamber. We also have no way to predict the amount of dye taken up and/or released by the sediments inside the housing. As the dye-dilution method relies on short term (1 hr) measurements and background corrections, the problems noted above are not usually an issue.

For manual injections and for a quick check on results while in the field, there are two simpler methods for determining flow rates. One method is to visually curve fit the field data against the flow absorbance curves predicted for a specific mixing chamber volume (see Assessment and Fig. 4). A second

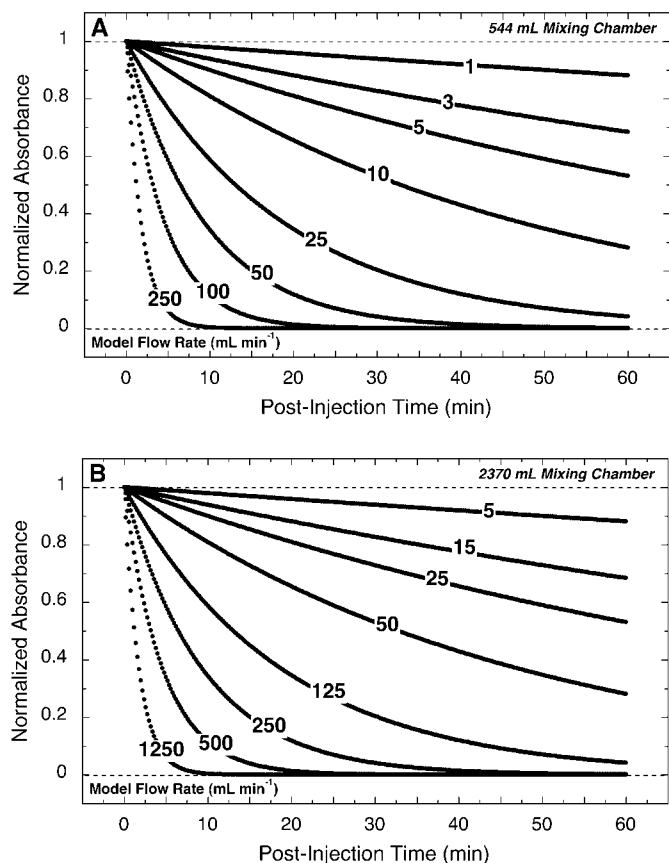


**Fig. 4.** Modeled dye dilution curves for various flow rates with dye mixing chambers of 2 volumes: A) 544 mL and B) 2370 mL. The post-injection time refers to time after the injection of dye into the dye-mixing chamber. Absorbance values are normalized to 1.0 absorbance units at  $t = 0$  min, and each dilution curve is labeled with the flow rate in  $\text{mL min}^{-1}$ .

method involves a simple mathematical representation of the dye-dilution plots in Fig. 4. This representation can take the form of a table that shows the change in background corrected absorbance as a function of time for a set of flow rates with a known dye-mixing chamber volume. For example, a flow rate of  $30 \text{ mL min}^{-1}$  ( $15 \text{ cm d}^{-1}$ ) would result in the absorbance decreasing by a factor of 1.74 over any 10 min period of time following an injection of dye into our 544 mL chamber. If the flow rate increases to  $40 \text{ mL min}^{-1}$  ( $20 \text{ cm d}^{-1}$ ), then this factor increases to 2.10.

When discussing the flow performance of the instrument, the volumetric unit of flow ( $\text{mL min}^{-1}$ ) is used. When discussing the field results, we use the unit of distance per time ( $\text{cm d}^{-1}$ ). This unit allows a direct comparison of flows for seepage meters with different surface area and a comparison of results from other study sites. Given our seepage housing surface area of  $0.286 \text{ m}^2$ ,  $1 \text{ mL min}^{-1}$  is equivalent to  $0.5 \text{ cm d}^{-1}$ .

### Assessment

To demonstrate the resolution of the flow rates by the dye-dilution method, we modeled the absorbance response under

various flow rates for the two mixing chamber volumes used in our field studies (544 mL in Fig. 4A and 2370 mL in Fig. 4B). In the model, time zero marks the initial dye injection, with the absorbance (background corrected) arbitrarily set to an initial value of 1.0. The model calculates new absorbance values of the water in the dye-mixing chamber at intervals of 0.2 min for a period of 1 h. The model assumes instantaneous homogenization of water within the mixing chamber for each time step.

The model results indicate that the 544 mL dye-mixing chamber can resolve flows that differ by  $\sim 1 \text{ mL min}^{-1}$  over a range of 1 to 10  $\text{mL min}^{-1}$  if one uses the absorbance measurements taken 20 to 60 min after a dye injection (Fig. 4A). Flows differing by 1 to 5  $\text{mL min}^{-1}$  over a range of 10 to 50  $\text{mL min}^{-1}$  can be resolved if one uses the absorbance measurements taken 10 to 30 min after a dye injection. Flow rates in the 25–100  $\text{mL min}^{-1}$  range can be determined with absorbance measurements taken 5 to 20 min after a dye injection. The resolution of the flow rates declines sharply with increasing flow. For example, flows greater than 200  $\text{mL min}^{-1}$  are poorly resolved with the 544-mL chamber. Because the flow resolution scales linearly with increasing volume, the 2370-mL mixing chamber, which is 4.4 times larger, extends the useful range five-fold to values greater than 1000  $\text{mL min}^{-1}$  (Fig. 4B). As expected, the larger chamber does not have the resolution of the smaller chamber at low flow rates. This chamber works best over the flow range of 10 to 200  $\text{mL min}^{-1}$  with absorbance measurements taken 20 to 40 min after a dye injection. Measurements over a 10–20 min period can be used to measure higher flows, albeit with a marked decline in resolution. With respect to the smaller chamber, the larger chamber also allows mid-range flows (10–60  $\text{mL min}^{-1}$ ) to be measured over a longer period of post-injection time (30–60 min.).

Our two dye-mixing chambers, including a recirculating pump, have been tested in the laboratory by measuring the change in absorbance as a function of time for different flow rates. Colorless tap water was pumped through a dye-filled chamber and the absorbance at 560 nm was measured manually using a laboratory spectrophotometer. In a bench top experiment with the 544-mL chamber, we demonstrated that the method could distinguish between flows of 45 and 50  $\text{mL min}^{-1}$  (Fig. 5). The decrease in absorbance over a period of 20 min is 1.4 times greater at flow rate of 50  $\text{mL min}^{-1}$  than at 45  $\text{mL min}^{-1}$ .

We compiled all our bench top calibrations of the 544-mL chamber ( $n = 34$ ) and compared the measured flow rate (using a graduated cylinder) with the model-derived value (Eq. 1; Fig. 6). These calibrations include both manual and automated (NAS-2E) absorbance measurements. The measured and calculated flow rates ranged from  $\sim 9$  to 90  $\text{mL min}^{-1}$  ( $\sim 5$ –45  $\text{cm d}^{-1}$ ) and fell along a straight line ( $R^2 = 0.99$ ) with a near 1:1 slope (slope = 1.02). These results indicate that the model (Eq. 1) is robust, and therefore, the instrument need not be periodically calibrated. In principle, the dye dilution method requires no calibration as one measures the relative change in absorbance in a known volume of water.

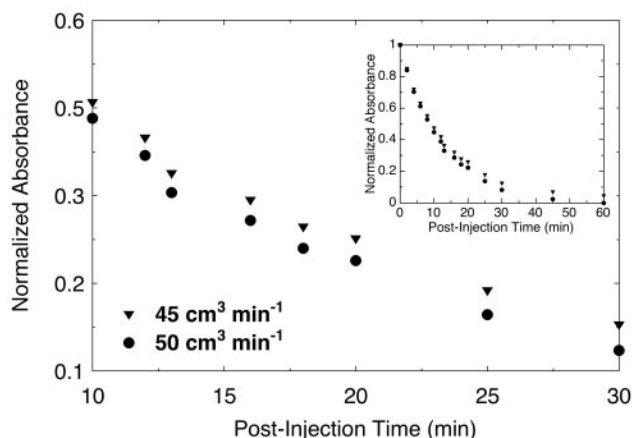


**Fig. 5.** A comparison of two bench top dye dilution experiments using the 544 mL mixing chamber, where the flow rate differed by only 5 mL min<sup>-1</sup> (equivalent to 2.5 cm d<sup>-1</sup>). The inset plot shows data for 60 min post injection, while the main figure has these data plotted for the 10–30 min time interval.

We also tested our new instrument in the field (Shelter Island site) against two other techniques. For one comparison, traditional seepage meter bags were attached to the end of the mixing chamber in order to record the volume of flow per unit time. Five consecutive half-hour bag deployments were carried out. Just prior to their use, air was squeezed out the bags. In the second comparison, a manual version of the dye-dilution method was carried out whereby a hand-held syringe was used to draw solutions out of the dye-injected mixing chamber at 10 min intervals over a period of an hour. This process was repeated and the solution absorbances were measured at 560 nm using an on-site laboratory spectrophotometer.

The dye-based flow rates, using both manual and automated methods, were in good agreement (11 vs. 12.5 and 6.5 vs. 5.5 cm d<sup>-1</sup>). However, the agreement between the automated dye method and the bag method was mixed. Two of the six comparisons were close, 33 versus 34 cm d<sup>-1</sup> and 25 versus 27 cm d<sup>-1</sup> for the dye-based and bag-based flow rates respectively. The other four comparisons (18 vs. 32, 25 vs. 32, 13 vs. 36, and 18 vs. 29 cm d<sup>-1</sup>) differed by factors of 1.3 to 2.8. The trend of bag flow exceeding dye-based flow suggests that, as dyed seepage water collects in the bag, there is active circulation of this water back into the mixing chamber. This would serve to suppress the dye-decay curve and therefore our estimate of flow (reduced slope = reduced flow). Our comparison was not meant to be a systematic and rigorous study of the two flow methods. This is best carried out in a test tank (Belanger and Montgomery 1992; Isiorho and Meyer 1999). Given the controversy surrounding the interpretation of seepage using bags (*see* Discussion), we can only speculate that a bag attached downstream of our mixing chamber affected the dye dilution curve by transforming our instrument's design from an open to a closed system.

This instrument has performed reliably in field tests at Waquoit Bay and Shelter Island, yielding hydrologically con-

sistent flow rates as well as revealing major and subtle connections between tidal stage and the rate and direction of submarine groundwater discharge. Field results are discussed next.

Shelter Island, located in Peconic Bay (Long Island, New York), was the site of a submarine groundwater discharge intercomparison experiment attended by a group of investigators using a variety of techniques. This intercomparison experiment took place between 17 and 24 May 2002 and was sponsored by Working Group 112 of the Scientific Committee on Oceanic Research. The group was charged with studying the magnitude of submarine groundwater discharge and its influence on coastal oceanographic processes. The experiment took place at a sandy beach in West Neck Bay, specifically site 1 in Fig. 9B of Paulsen et al. (2001).

Our instrument was deployed at two locations for 2.7 d and 2.5 d respectively. The “inshore” deployment (17 May 2002–20 May 2002) was located approximately 10 m seaward of mean tide. Several of the low tides exposed our instrument to air as the seawater completely receded. Exposure to air and servicing resulted in gaps in the time-series flow data (Fig. 7). Rivulets of freshwater flowed down the face of the beach to the bay during these low tides. The “offshore” deployment (20 May 2002–22 May 2002) took place 10 m further to sea; the water was 1.5 m deep at high tide and the instrument remained underwater at low tide. Given the limited time of the experiment, only 2 h elapsed between seepage housing installation and the commencement of the flow measurements.

During the course of two deployments, our instrument produced over 4 d of hourly flow data, which ranged from ~2–40 cm d<sup>-1</sup>. Both deployments yielded a set of flow rates that were consistent with respect to their tidal dependency (Fig. 7). Whereas the direction of flow remained out of the

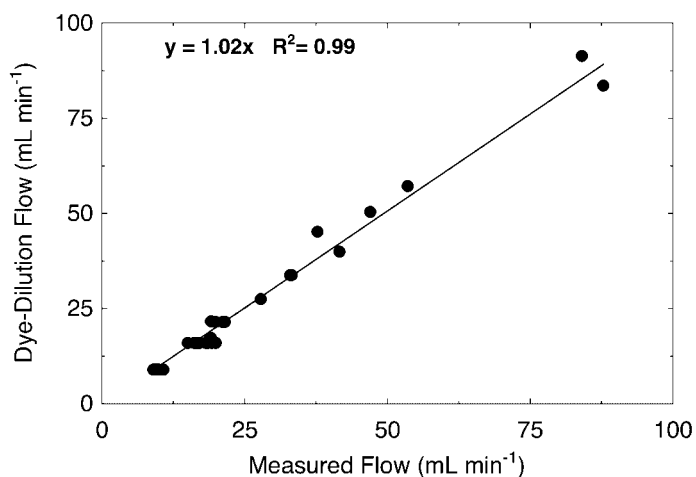


**Fig. 6.** Laboratory comparison of the measured flow rate (using a graduated cylinder) with the model-derived value (Eq. 1) for the dye dilution method using the 544 mL mixing chamber. Flow rate was adjusted by a peristaltic pump attached to a container of freshwater. Absorbance measurements were made every five min for 1 h post-injection.

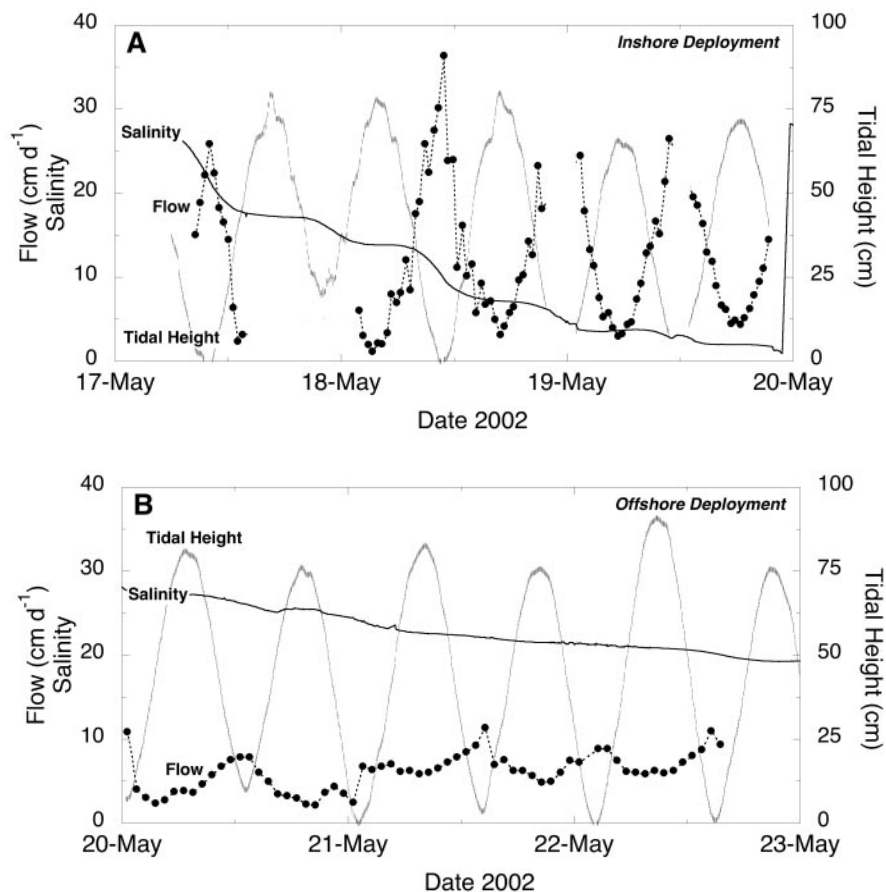


**Fig. 7.** Seepage time-series from Shelter Island collected in May 2002. The top panel is data collected from an inshore location; the bottom panel is an offshore deployment. Dye injections were performed every 30 min, with absorbance measurements collected with 2 min resolution. The salinity from within the seepage housing and the tidal height at the location of the deployment also are shown.

sediment throughout the two deployments, there was a strong negative correlation between the magnitude of the flow rate and the tidal stage. The maximum flow occurred at low tide and minimum flow occurred at high tide, as previously observed by Paulsen et al. (2001) for the same seepage face. The inshore site was characterized by a much greater magnitude and range of seepage flow than the offshore site. The high and low flow rates at the inshore site were 37 and 2 cm d<sup>-1</sup>, respectively as compared with 12 and 3 cm d<sup>-1</sup> at the offshore site. From the calculated uncertainty on the dye-decay curves, the error on the flow rates was ~1 cm d<sup>-1</sup>, which is quite small relative to the absolute flow rates (Fig. 7).

Although the flow rates at the offshore site are low (3–13 cm d<sup>-1</sup>), our instrument was able to resolve small differences driven by the tide. This was the case even though the large (2370 mL) mixing chamber, not intended for measuring such low flows (Fig. 4B), was used for this deployment. Our smaller mixing chamber would have been better suited to measuring the small changes in absorbance that resulted from the dilution of dye with discharging water.

The salinity data provide a valuable insight into the composition of SGD to the two sites. Whereas the salinity of the ambient seawater (not shown) remained constant at 28 for the offshore deployment and for most of the inshore deployment, the internal salinity on both deployments decreased as function of time (Fig. 7). The largest decrease, from 28 to 2 in 2.7 d, occurred at the inshore site. In contrast, the internal salinity at the offshore site decreased from 28 to 19 over 2.5 d. The decrease in salinity to almost zero at the inshore site indicates that the source of SGD to this site was freshwater. If one assumes a seepage housing head-space volume of ~30 L, a groundwater end-member salinity of 0, and mean flow rate of 15 cm d<sup>-1</sup> as measured by our instrument (Fig. 7), then a two-end member dilution model, similar to the one used in Fig. 4, predicts that the internal salinity will decrease from 28 to 2 over 2.7 d. This predicted decrease in salinity agrees with our observed decrease and reinforces our conclusion that the SGD at the inshore site is freshwater. The discharge of freshwater at the inshore site is consistent with conductivity probe measurements made

across the seepage face as part of the May 2002 intercomparison study (Stieglitz pers. comm.).

The slower rate of decrease in the internal salinity at the offshore site could reflect two processes: reduced freshwater flow or subsurface entrainment of seawater during SGD. A dilution model (as above) using a freshwater end member rules out the first explanation. Assuming that the seepage water had a salinity of 0 and mean flow rate of  $5 \text{ cm d}^{-1}$  as measured by our instrument (Fig. 7), then a dilution model predicts that the salinity will decrease to 12 at 2.5 d (compared with the observed salinity decrease to 19). To match the observed decrease in salinity, the dilution model requires the end-member fluid to have a salinity of  $\sim 10\text{--}12$ . Thus, the salinity data indicate that the outflow of water at the offshore site is a mixture of freshwater and seawater. This conclusion is consistent with conductivity probe measurements that indicated that the pore waters of the sediments under our offshore site were brackish (Stieglitz pers. comm.).

The main feature of the Waquoit Bay flow data is the tidal dependence of SGD. With only a few notable exceptions, the flow direction was inversely related to the stage of the tide. Unlike the Shelter Island site where the flow is always out of the sediments, the flow direction at the Waquoit Bay site reversed from net outflow to net inflow during the transition from low to high tide. The maximum outflow was  $47 \text{ cm d}^{-1}$  whereas the maximum inflow was  $\text{cm d}^{-1}$ .

Waquoit Bay is a shallow estuary located on the south shoreline of Cape Cod, Massachusetts; a map of the bay can be found in Charette et al. (2001). A significant portion of the freshwater input to the bay occurs as submarine groundwater discharge (Valiela et al. 1990; Cambareri and Eichner 1998; Charette et al. 2001). SGD measurements using Lee-type seepage meters with the bag method have shown that SGD is most pronounced in a narrow ( $\sim 25 \text{ m}$ ) band along the head of the bay (Michael et al. 2001). The spatial variability in the rate of SGD to the head of the bay is large in both the long shore and cross-shore directions (Michael et al. 2001).

A three-week deployment took place from 24 August 2002–8 September 2002 at a site about 5 m below mean low tide (Fig. 8). Gaps in the time-series data in early September reflect a period of instrument maintenance. The instrument remained submerged throughout the deployment and flow measurements were collected hourly. The time-series encompassed one complete neap to spring tidal transition. The peak neap tide occurred 30 August 2002 and peak spring tide was 7 September 2002. The bay salinity at the deployment site was fairly constant throughout the whole deployment at  $\sim 28\text{--}30$ . The internal salinity ranged from 27 to 31 over the same time period. The presence of both inflow and outflow creates salinity equilibrium between the seepage housing and the bay. Thus, internal salinity does not allow us to estimate the salinity of SGD at this location.

A more detailed look at the time-series data reveals several important features (Fig. 9). Our instrument was able to record

even the most subtle connections between the flow rate and tidal stage: even the shoulders and dips in tidal height during rising tides were accompanied by shoulders and dips in the seepage rates. While these changes in the seepage rate are small ( $1\text{--}3 \text{ cm d}^{-1}$ ), they were measurable and repeatable features of the time series. While simulations of the dye-dilution method (Fig. 4) indicate that changes of  $1\text{--}3 \text{ cm d}^{-1}$  should be measurable, the Waquoit Bay time-series reveals the ability of our instrument to pick up these subtle variations under field conditions.

As noted earlier, the majority of high tides in the three-week experiment were characterized by inflow. However, this was not true for the high tides on the mornings of 30 and 31 August 2002. On these days, the instrument recorded outflow during the complete tidal cycle (Fig. 8). Although the rate of outflow decreased as the tide increased, the flow never shifted direction. Interestingly, this feature coincided with the neap tide where the high tide level was the lowest of the entire time series. This result suggests that the high tide on these days never exceeded the elevation of the water table beneath the beach face.

## Discussion

As discussed in numerous articles, the volumetric measurement of a seepage rate using a bag on the end of a seepage housing is prone to artifacts (Shaw and Prepas 1989; Belanger and Montgomery 1992; Isiorho and Meyer 1999; Shinn et al. 2002). Specifically, bag-derived flow rates may be biased by constriction of flow by the bag and/or by wave-induced motion of the water inside the bag. Bags, partially prefilled with water prior to deployment, yielded more accurate results than empty bags (Belanger and Montgomery 1992). Moreover, the intensive labor involved in the bag method does not lend itself to time series studies on the scale of lunar tidal cycles and seasons. Perhaps most importantly, the validity of reverse flow measurements using bags has not been adequately proven. For the reasons mentioned above, the development of automated seepage meters have been carried out by several groups. A heat-pulse based instrument has been developed by Taniguchi and Fukuo (1993) and Taniguchi and Iwakawa (2001). The timed transmission of heat pulses to downstream thermistors in a flow tube forms the basis of this method. The Krupa-type seepage meter also employs heat-pulse technology (Krupa et al. 1998). Paulsen et al. (2001) have developed an acoustic (ultrasonic) automated seepage meter, based on the timed perturbation of sound in a moving fluid. Our instrument uses the timed dilution of dye as the basis for calculating the flow. All three instruments use seepage housings to collect and focus the flow through a tube or small chamber. All three instruments employ an “open-system” design that allows unrestricted fluid flow in either direction.

We compared the design and measurement properties of the three types of automated seepage meters (Table 1). All three instruments are similar with respect to their time-resolving capability and flow rate sensitivity. Whereas the acoustic sensor is capable of making flow measurements with a resolution of 1 s to 5 min, data on such short time scales are not

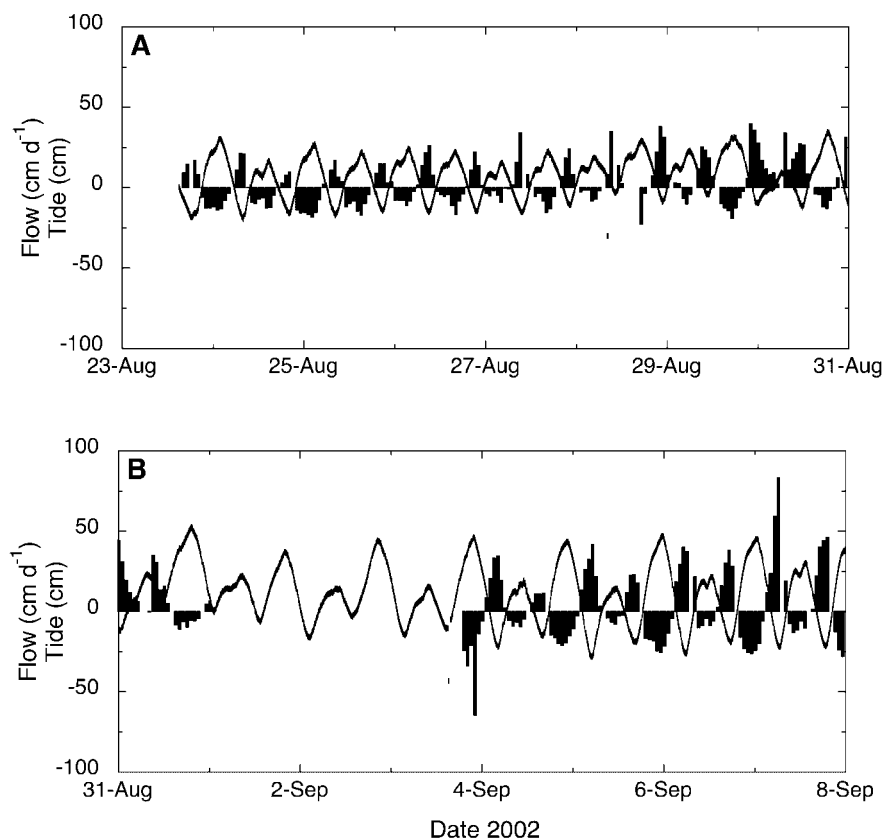


**Fig. 8.** Seepage flow time-series from Waquoit Bay collected in August–September 2002. Dye injections were performed hourly, with absorbance measurements collected with 2 min resolution for 30 min post injection. Positive and negative values refer to flow out of and into the sediments respectively. The tidal height at the location of the deployment is also shown.

usually required for the study of flow into and out of sediments. All three instruments cover a wide range of flows encountered in marine and freshwater systems and can be modified to measure high ( $100\text{--}1000\text{ cm d}^{-1}$ ) flow rates by using a seepage housing with a smaller surface area. One advantage of the dye-dilution instrument is that the working range of flow measurement can easily be altered by swapping dye-mixing chambers of different volumes (Figs. 4, 5). For example, very slow ( $<0.1\text{ cm d}^{-1}$ ) and very fast ( $>300\text{ cm d}^{-1}$ ) rates could be measured by using small (100 mL) and large (4000 mL) mixing chambers. Even extremely slow rates of discharge, such as those observed in the benthic ocean and hydrothermal vents (Sayles and Dickinson 1991; Tryon et al. 2001), could be measured by using a very small volume-mixing chamber in a dye dilution system. This application would be analogous to the chemical tracer dilution technique used in the automated seepage meter of Tryon et al. (2001).

The dye-dilution and the acoustic instruments are capable of measuring bi-directional flow, as would be the heat-pulse instrument with an additional thermistor mounted upstream of the heat-pulse generator. This advantage is critical in studies of coastal regions where interplay between water table elevation and tidal height can drive the seepage into the sedi-

ments as shown by our experiments and Paulsen et al. (2001). The ability of all three instruments to collect flow data for several weeks allows a closer look at the relationship between daily and monthly lunar cycles, water table elevation and SGD (Robinson et al. 1998; Paulsen et al. 2001; Taniguchi and Iwakawa 2001; Taniguchi 2002; this article).

Unlike the other two instruments, the dye-dilution method can be operated in manual mode. In practice, this requires the recirculating pump, its battery pack and the dye-mixing chamber but not the NAS unit, which contains the automated dye injector and spectrometer (Figs. 1, 3). By hand, the operator would inject dye into the mixing chamber and collect aliquots of water from the mixing chamber on a timed basis. The absorbances of these aliquots could be measured with an inexpensive spectrophotometer and used to determine the flow rates in the field. This method is less labor intensive than the bag method, and has the major advantage of detecting and accurately quantifying reverse flow. The equipment needed to turn a seepage housing into a manually operated dye-dilution based flow instrument would cost less than \$1500. In-situ analyzers, such as our NAS-2E model, add about \$20,000 to the cost.

In conclusion, the time-series data from Shelter Island and Waquoit Bay are very encouraging with respect to the capabil-

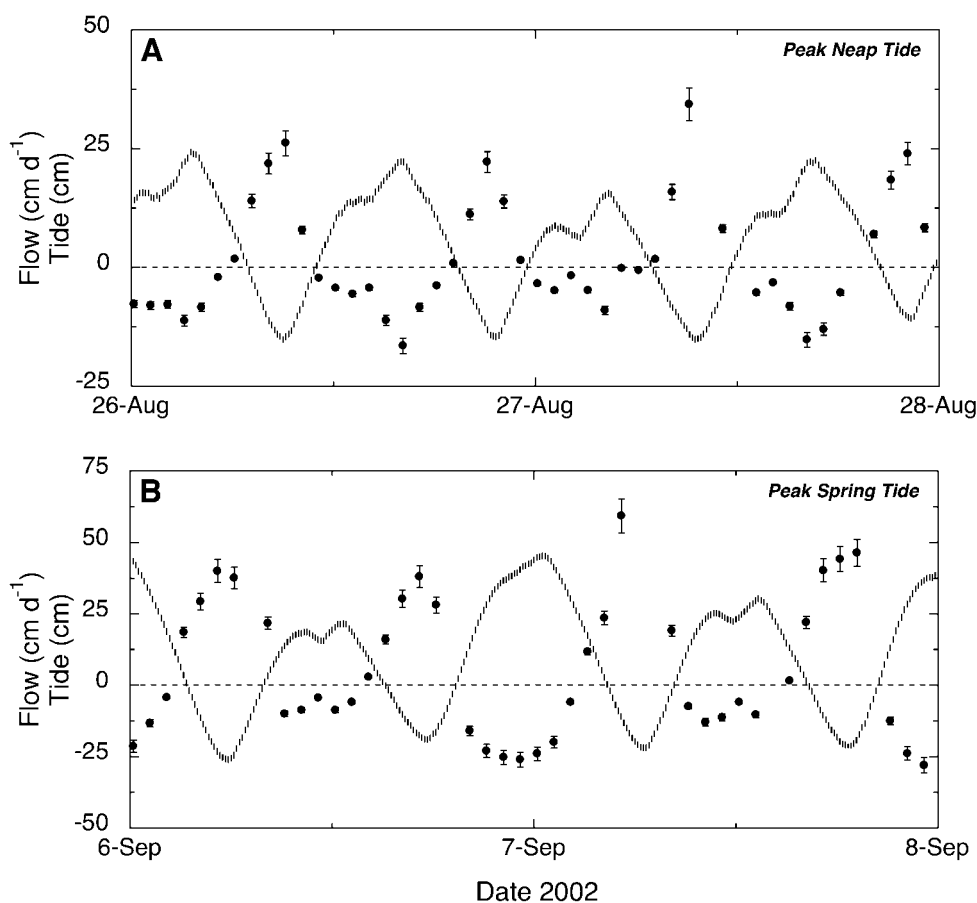


**Fig. 9.** Seepage flow time-series from Waquoit Bay collected in August–September 2002 focused on 2 d surrounding peak neap tide (A) and peak spring tide (B). Note change in scale on y-axis. Flow (●) is in  $\text{cm d}^{-1}$ , tidal height (vertical line) is in cm. Error bars represent the standard error (1-sigma) of the slope fit to the dye-dilution curve.

ities of our new automated seepage meter. The dye-dilution method is versatile in being able to measure a wide range of flow rates in two directions. The instrument has yielded hydrologically consistent flow rates and has revealed major and subtle connections between tidal stage and the rate and direction of submarine groundwater discharge. The magnitude of the outflow at both sites is inversely correlated with the tidal height. In Waquoit Bay, the flow direction switches from outflow to inflow at the transition low to high tide. The addition of sensors to record changes in salinity inside and outside of the seepage housing provides valuable information on the sources of submarine groundwater discharge to the coastal ocean (freshwater and brackish water to the inshore and offshore sites at Shelter Island and predominately recirculated seawater to the Waquoit Bay site).

### Comments and recommendations

Key components of the hardware and software on our instrument can be modified to match the flow conditions of the site and the desired sampling conditions of the user. Seepage housings of different surface areas and dye-mixing cham-

bers of different volumes can be used. In practice, using mixing chambers of different volumes is a far less expensive means of optimizing the instrument to the flow rates (Fig. 4). Also, the user can set the frequency of dye injection and the frequency of absorbance measurements according to the flow conditions. With respect to the latter, the user can decide how frequently to measure the absorbance in the dye-mixing chamber and at the inlet and outlet ports (Fig. 1). As the two ports serve to determine the background absorbance of the outflow and inflow water, we typically sample them less frequently than we do the dye-mixing chamber. If the study area was determined to have water that flows out only, then the outlet port on the mixing chamber need not be sampled.

The choice of chamber volume allows the operator to measure flow rates over a large dynamic range. To approach the optimal measurement conditions, a dye-mixing chamber with a volume appropriate to the flow rate needs to be used. If the dye-injected solution is flushed out too quickly due to a high flow, then there will not be sufficient time to make a series of absorbance measurements. Conversely, if the dye is flushed out too slowly due to low flow, then the change of absorbance

**Table 1.** Comparison of automated seepage meters

	Acoustic	Heat pulse	Dye dilution
Reference	Paulsen et al. 2001	Taniguchi et al. 1993	This article
Area of seepage housing (m <sup>2</sup> )	0.21, can be changed	0.20, can be changed	0.29, can be changed
Diameter of flow tubing (cm)	0.95	1.1	0.85
Time resolution of flow measurement			
Minimum	1 s	5 min	5 min
Maximum	Adjustable: up to days	Adjustable: up to days	Adjustable: up to days
Range of measurable flow rates (cm d <sup>-1</sup> )	0.9–300	2–40	0.5–150*
Able to measure forward and reverse flow	Yes	Not in current configuration†	Yes
Able to operate manually	No	No	Yes

\*Adjustable to lower and higher values

†Requires a second set of thermistors and electronics

with time will be small and subsequent injections of dye will build up in the dye-mixing chamber leading to off-scale absorbance values. Our 2370-mL chamber would be most applicable where the flow rates cover 10–200 mL min<sup>-1</sup> (5–100 cm d<sup>-1</sup>). Our 544 mL chamber works best at slower flows (1–50 mL min<sup>-1</sup> or 0.5–25 cm d<sup>-1</sup>), more typical of seepage rates observed in marine, estuarine and freshwater systems (Lee 1977; Bokuniewicz 1980; Lewis 1987; Taniguchi and Fukuo 1993; Boyle 1994; Robinson et al. 1998; Paulsen et al. 2001; Taniguchi 2002).

The time-resolution of the flow measurement can be set by frequencies of dye injection and absorbance measurements. Using the NAS-2E analyzer, extracting a water sample and making an absorbance measurement from each of three ports takes less than 2 min. Hence, a cycle of one absorbance value for all three sampling locations requires about 6 min. The sampling frequency can be reduced to < 1 min if one only monitors the water in the dye-mixing chamber water; this protocol does not involve moving the motor-driven syringe valve. To determine the flow rates on an hourly basis, we typically employ a program that spans ~30 min of measurements followed by 30 min of inactivity; thus, each flow measurement represents an average of flow over the 30-min program. The first ~6 min of the program are dedicated to measuring background from the three ports. Then, dye is injected followed by ~20 min of absorbance measurements ( $n = 20$ ) from the mixing chamber (Port B); these are the measurements that form the dye-decay curve. Lastly, midway through the 20-min mixing chamber cycle, background absorbance samples are drawn and analyzed from the inlet and outlet ports (Fig. 1); these measurements establish the direction of flow. As noted earlier, the software on the NAS-2E allows operators to design their own injection and sampling protocols.

Before collecting samples from any type of seepage meter, the usual procedure is to push the seepage housing into the sediment and wait several days for settling and sealing to take place. Once this equilibration period is completed, the other components of our instrument are put in place. Batteries are connected, the pump is turned on and the NAS-2E is pro-

grammed to start its injection and analysis sequence. Though the instrument is entirely self-contained, the absorbance data for segments of a long deployment can be retrieved without removing the whole the instrument from the sediment. This is accomplished by connecting a laptop PC to the NAS with a watertight cable, downloading the data and restarting the program. In practice, we do this every 3–5 d.

As described in Materials and procedures, if dye builds up to unacceptably high concentrations in the headspace of the seepage housing, then it may not be possible to background correct the absorbances recorded in the dye-mixing chamber. This problem has arisen on occasion in our more recent studies of Waquoit Bay. Solutions include reducing the amount and frequency of dye injected and/or flushing out the headspace water with ambient water.

No filters are used on any of inlets or outlets as they would impede the flow water. Hence, algae and small particles enter the dye-mixing chamber and can cause problems by fouling the spectrometer cell and by affecting the absorbance of light. In practice, most particles settle on the bottom of the mixing chamber and light scattering by particles in the spectrometer doesn't appear to be significant problem. We recently added a second reagent bag containing a 10% solution of household bleach to the NAS-2E analyzer and have modified the software to inject this bleach into the spectrometer cell after each flow measurement. As indicated by the spectrometer's transmission data, this new protocol appears to keep the cell walls much cleaner.

## References

- Basu, A. R., S. B. Jacobsen, R. J. Pored, C. B. Dowling, and P. K. Aggarwal. 2001. Large groundwater strontium flux to the oceans from the Bengal Basin and the marine strontium isotope record. *Science* 293: 1470-1473.
- Belanger, T. V., and M. T. Montgomery. 1992. Seepage meter errors. *Limnol. Oceanogr.* 37: 1787-1795.
- Bokuniewicz, H. 1980. Groundwater seepage into Great South Bay, New York. *Estuar. Coast. Mar. Sci.* 10: 437-444.
- . 2001. Toward a coastal ground-water typology. *J. Sea Res.* 46: 99-108.

- Boyle, D. R. 1994. Design of a seepage meter for measuring groundwater fluxes in the nonlittoral zones of lakes—evaluation in a boreal forest lake. *Limnol. Oceanogr.* 39: 670-681.
- Burnett, W. C., M. Taniguchi, and J. Oberdorfer. 2001. Measurement and significance of the direct discharge of groundwater into the coastal zone. *J. Sea Res.* 46: 109-116.
- Burnett, W., J. Chanton, J. Christoff, E. Kontar, S. Krupa, M. Lambert, W. Moore, D. O'Rourke, R. Paulsen, C. Smith, L. Smith, and M. Taniguchi. 2002. Assessing methodologies for measuring groundwater discharge to the ocean. *EOS Trans. AGU* 83: 117.
- Cambareri, T. C., and E. M. Eichner. 1998. Watershed delineation and ground water discharge to a coastal embayment. *Ground Water* 36: 626-634.
- Charette, M. A., K. O. Buesseler, and J. E. Andrews. 2001. Utility of radium isotopes for evaluating the input and transport of groundwater-derived nitrogen to a Cape Cod estuary. *Limnol. Oceanogr.*, 46: 465-470.
- Krest, J. M., W. S. Moore, L. R. Gardner, and J. T. Morris. 2000. Marsh nutrient export supplied by groundwater discharge: Evidence from radium measurements. *Global Biogeochem. Cyc.* 14: 167-176.
- Krupa, S. L., T. V. Belanger, H. H. Heck, J. T. Brok, and B. J. Jones. 1998. Krupaseep—the next generation seepage meter. *J. Coastal Res.* 25: 210-213.
- Ishorho, S., and J. H. Meyer. 1999. The effects of bag type and meter size on seepage meter measurements. *Ground Water* 37: 411-413.
- Johannes, R. E. 1980. The ecological significance of the submarine discharge of groundwater. *Marine Ecology* 3: 365-373.
- , and C. J. Hearn. 1985. The effect of submarine groundwater discharge on nutrient and salinity regime in a coastal lagoon off Perth, Western Australia. *Estuar. Coast. Shelf Sci.* 21: 789-800.
- Lee, D. R. 1977. A device for measuring seepage flux in lakes and estuaries. *Limnol. Oceanogr.* 22: 140-147.
- Lewis, J. B. 1987. Measurements of groundwater seepage flux onto a coral reef: spatial and temporal variations. *Limnol. Oceanogr.* 32: 1165-1169.
- Li, L., D. A. Barry, F. Stagnitti, and J.-Y. Parlange. 1999. Submarine groundwater discharge and associated chemical input to a coastal sea. *Water Resources Res.* 35: 3253-3259.
- Michael H. A., M. A. Charette, J. Lubetsky, and C. Harvey. 2001. Assessing rates and mechanisms of submarine groundwater discharge: a combined approach using seepage meters and radium. *EOS Trans. AGU* 82: 153.
- Millham, N. P., and B. L. Howes. 1994. Freshwater flow into a coastal embayment: Groundwater and surface water inputs. *Limnol. Oceanogr.* 39: 1928-1944.
- Montlucon D., and S.A. Sanudo-Wilhelmy. 2001. Influence of net groundwater discharge on the chemical composition of a coastal environment: Flanders Bay, Long Island, New York, *Environ. Sci. Technol.* 35: 480-486.
- Moore, W.S. 1996. Large groundwater inputs to coastal waters revealed by  $^{226}\text{Ra}$  enrichments. *Nature* 380: 612-614.
- . 1999. The subterranean estuary: a reaction zone of ground water and seawater. *Mar. Chem.* 65: 111-125.
- , and T. J. Shaw. 1998. Chemical signals from submarine fluid advection onto the continental shelf. *J. Geophys. Res.* 103: 21543-21552.
- Paulsen, R. J., C. F. Smith, D. O'Rourke, and T.-F. Wong. 2001. Development and evaluation of an ultrasonic ground water seepage meter. *Ground Water* 39: 904-911.
- Reay, W. G., D. L. Gallagher, and G. M. Simmons, Jr. 1992. Groundwater discharge and its impact on surface water quality in a Chesapeake Bay Inlet. *Water Resources Bull.* 28: 1121-1134.
- Robinson, M., D. Gallagher, and W. Reay. 1998. Field observations of tidal and seasonal variations in ground water discharge to tidal estuarine surface water. *Ground Water Monitor. Remediat.* 18: 83-92.
- Rutkowski, C. M., W. C. Burnett, R. L. Iverson, and J. P. Chanton. 1999. The effect of groundwater seepage on nutrient delivery and sea grass distribution in the north-eastern Gulf of Mexico. *Estuaries* 22: 1033-1040.
- Sayles, F. L., and W. H. Dickenson. 1991. The Seep Meter: a benthic chamber for sampling and analysis of low velocity hydrothermal vents. *Deep-Sea Res.* 38: 129-141.
- Shaw, R. D., and E. E. Prepas. 1989. Anomalous, short term influx of water into seepage meters. *Limnol. Oceanogr.* 34: 1343-1351.
- Shaw, T. J., W. S. Moore, J. Klopfer, and M. A. Sochaski. 1998. The flux of barium to the coastal waters of the southeastern United States: the importance of submarine groundwater discharge. *Geochim. Cosmochim. Acta.* 62: 3047-3052.
- Shinn, E. A., C. D. Reich, and T. D. Hickey. 2002. Seepage meters and Bernoulli's revenge. *Estuaries* 25: 126-132.
- Simmons Jr., G. M. 1992. Importance of submarine groundwater discharge (SGWD) and seawater cycling to the material flux across sediment/water interfaces in marine environments. *Mar. Ecol. Prog. Ser.* 84: 173-184.
- Taniguchi, M. 2002. Tidal effects on submarine groundwater discharge into the oceans. *Geophys. Res. Lett.* 10.1029/2002GL014987, 2-1-2-3.
- , and Y. Fukuo. 1993. Continuous measurements of ground-water seepage using an automatic seepage meter. *Ground Water* 31: 675-679.
- , M., and H. Iwakawa. 2001. Measurement of submarine groundwater discharge rates by a continuous heat-type automated seepage meter in Osaka Bay, Japan. *J. Groundwater Hydrol.* 43: 271-277.
- Tobias, C. R., S. A. Macko, I. C. Anderson, E. A. Canuel, and J. W. Harvey. 2001. Tracking the fate of high concentration groundwater nitrate plume through a fringing marsh: a combined groundwater tracer and in situ enrichment study. *Limnol. Oceanogr.* 46: 1977-1989.
- Tryon, M., K. Brown, L. Dorman, and A. Sauter. 2001. A new

- benthic aqueous flux meter for the very low to moderate discharge rates. *Deep-Sea Res.* 48: 2121-2126.
- Uchiyama, Y., K. Nadaoka, P. Rolke, K. Adachi, and H. Yagi. 2000. Submarine groundwater discharge into the sea and associated nutrient transport in a sandy beach. *Water Resour. Res.* 36: 1467-1479.
- Valiela, I., J. Costa, K. Foreman, J. M. Teal, B. Howes, and D. Aubrey. 1990. Transport of groundwater-borne nutrients from watersheds and their effects on coastal waters. *Biogeochem.* 10: 177-197.
- , K. Foreman, M. LaMontagne, D. Hersh, J. Costa, P. Peckol, B. DeMeo-Anderson, C. D'Avanzo, M. Babione, C. H. Sham, J. Brawley, and K. Lajtha. 1992. Couplings of watersheds and coastal waters: Sources and consequences of nutrient enrichment in Waquoit Bay, Massachusetts. *Estuaries* 15: 443-457.
- Zimmerman, C. F., J. R. Montgomery, and P. R. Carlson. 1985. Variability of dissolved reactive phosphate flux rates in nearshore estuarine sediments: effects of groundwater flow. *Estuaries* 8: 228-236.

*Received 3 March 2003*

*Revised 21 May 2003*

*Accepted 23 May 2003*